MULTI-OBJECTIVE OPTIMIZATION FRAMEWORK FOR MATERIAL AND STRUCTURAL DESIGN: AN APPLICATION TO PERMANENT-FORMWORK-INTEGRATED REINFORCED CONCRETE BEAM

Minh Hai Nguyen[1]*, Hoang Nam Phan[1], Cong Chanh Doan[1,2], Van Phuc Ha[1], Duy Vu Vo[1], Cong Tien Ho[3], Phuong Nam Huynh[1], Viet Hai Do[1]

[1]The University of Danang - University of Science and Technology, Vietnam
[2]Tra Vinh University, Vietnam
[3]Danang Architecture University, Vietnam

*Corresponding author: nmhai@dut.udn.vn

(Received: January 24, 2026; Revised: March 15, 2026; Accepted: March 25, 2026)

DOI: 10.31130/ud-jst.2026.24(3).064E

Abstract - Multi-objective optimization methods are increasingly important in construction design, where technical, economic, and environmental criteria must be balanced. This paper presents an overview of a multi-objective optimization framework to support decision-making at the preliminary design stage. The framework comprises three main steps: (i) developing predictive models for each performance indicator; (ii) defining design scenarios and constraints; and (iii) applying optimization algorithms to identify solution sets that enable preference-based selection. A representative case study on the design of reinforced concrete beams with precast permanent formwork is also introduced, in which structural capacity, cost, and carbon emissions are simultaneously considered. The results demonstrate that the framework effectively identifies optimal solutions while elucidating trade-offs among criteria, thereby supporting context-specific design decisions. The proposed approach shows strong potential for broader application to other design problems, particularly with advances in big-data analytics and the growing urgency of integrating Net Zero objectives in the construction sector.

Key words - Multi-objective optimization; NSGA-II; Reinforced concrete beam; Precast permanent formwork; Sustainable structural design; Carbon emission assessment

1. Introduction

In recent years, the construction industry has witnessed a marked shift from traditional single-objective design thinking toward multi-objective optimization (MOO), reflecting the increasingly complex demands of modern construction projects. Structures are required not only to satisfy strength and durability requirements, but also to ensure constructability, optimize life-cycle costs, and reduce environmental impacts in line with the sustainable development orientation of the construction sector [1, 2]. Balancing these criteria within a single design solution gives rise to multi-objective problems involving technical, economic, and environmental constraints that may conflict with one another.

Several studies have shown that optimizing a single objective often leads to compromised performance in other aspects [3]. For example, maximizing structural capacity may increase costs and CO_2 emissions, whereas minimizing cost may adversely affect durability or service life. Moreover, objectives are often addressed sequentially, starting with the optimization of one criterion and then proceeding to the next based on the obtained results. If any objective fails to meet the requirements at a given stage, the entire design process must be restarted from the beginning. This not only prolongs the design time but also requires redefining the input conditions, resulting in costly iterations, particularly when additional experimental validation is needed, and reducing the overall efficiency of the design process.

In contrast, MOO enables the identification and analysis of trade-offs among competing objectives through Pareto-optimal solution sets [4]. In structural engineering, MOO has been applied to optimize geometry, structural configurations, reinforcement layouts, as well as life-cycle costs and risk resilience [5–7]. In materials engineering, MOO supports the optimization of concrete mix designs and novel materials by simultaneously considering mechanical performance, workability, durability, and environmental criteria [8, 9]. Furthermore, while earlier studies often relied on analytical or linear regression models to predict individual performance indicators, approaches that struggle to accurately capture the nonlinear and high-dimensional relationships inherent in experimental and structural data, the recent development of machine learning techniques such as Gene Expression, Random Forest, and Support Vector Regression has enabled more accurate and flexible predictive modeling, thereby improving optimization quality [10].

Against this background, this report first presents a general overview of the MOO framework as applied to structural and construction material design, emphasizing the potential of integrating predictive models derived from experimental data, analytical analysis, or machine learning. This overview aims to provide readers with a broader perspective on multi-objective optimization design, thereby facilitating the flexible development of ideas for specific design problems under various contexts. Subsequently, to further illustrate the practical application of the approach, a representative case study is conducted on the design of reinforced concrete beams using permanent formwork, in which flexural capacity, cost, and CO_2 emissions are simultaneously considered. The report is expected to provide a scientific and technical foundation for the systematic implementation of MOO, in line with current trends toward integrated multi-objective design for more sustainable construction.

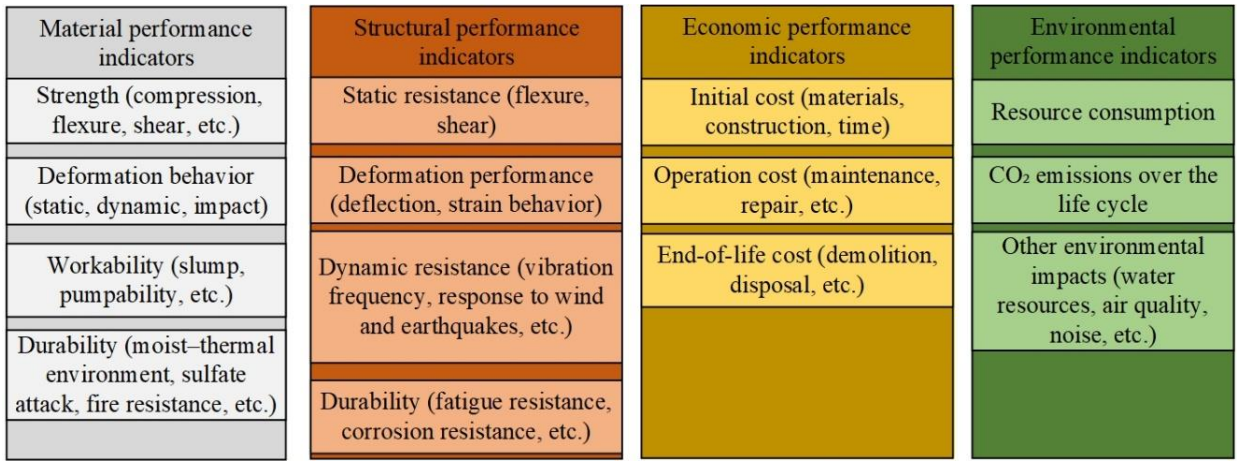

a) Typical objectives in materials and structural design

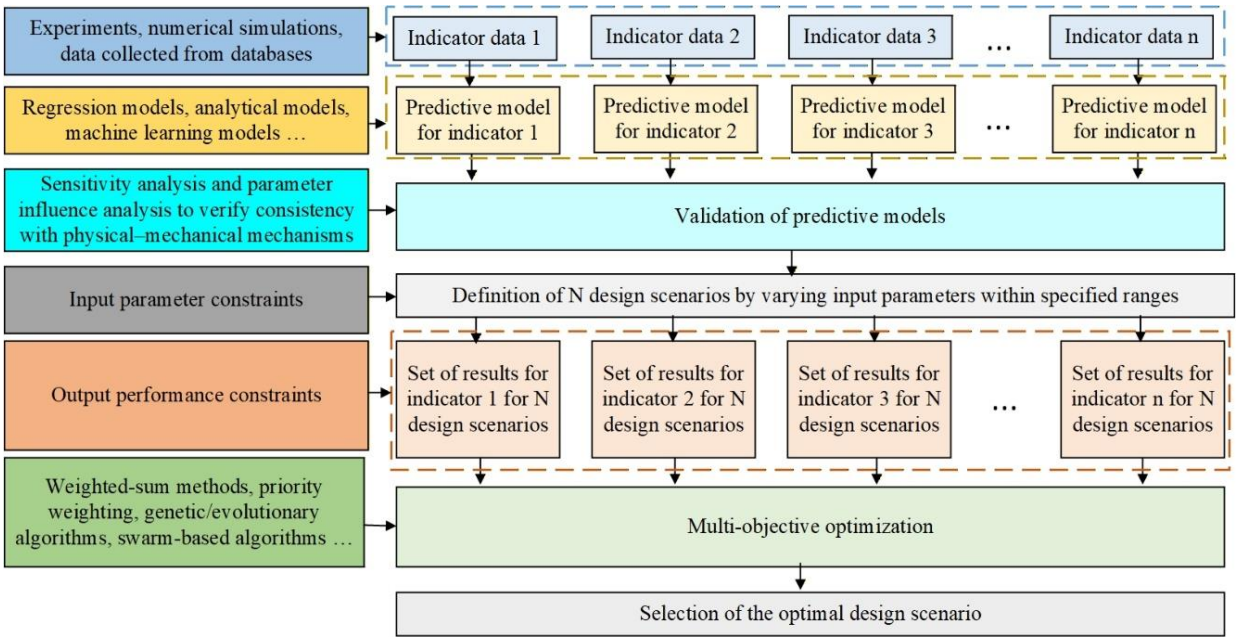

b) Multi-objective optimization design framework

Figure 1. *Overview of the multi-objective optimization design framework*

2. Overview of the multi-objective optimization framework

2.1. Overview

In material and structural design within the construction field, several typical groups of performance indicators can be classified into four main clusters, as illustrated in Figure 1(a). The material performance cluster includes mechanical properties such as compressive, flexural, and shear strength; deformation behavior under static or dynamic conditions; mixture workability; and durability against environmental, chemical, or thermo-hygrometric actions. The structural performance cluster reflects the overall load-bearing capacity through static and dynamic resistance, deformation levels, and the ability to withstand fatigue and corrosion throughout the service life. The economic performance cluster comprises initial costs (materials, construction, and time), operational costs (maintenance and repair), and end-of-life costs related to demolition, recycling, or disposal. The environmental performance cluster addresses resource consumption, life-cycle CO_2 emissions, and other impacts such as effects on water resources, air quality, and noise. These indicators can be further extended to encompass other areas of the construction sector, such as geotechnical engineering, hydraulic engineering, or transportation infrastructure.

Simultaneously optimizing all of the above indicators is considered ideal in construction design. In practice, however, few projects can account for the full set of criteria, as doing so requires extensive databases and significant computational effort. This is even less feasible when adopting traditional single-objective design approaches. In such cases, if any criterion is not satisfied, nearly all initial design parameters must be redefined, forcing the entire design process to restart, which substantially increases both time and cost. Moreover, some criteria may be inherently conflicting. For instance, enhancing structural load-bearing capacity typically requires increased material usage, leading

to higher costs and carbon emissions. Therefore, there is an urgent need for a more comprehensive design framework capable of identifying balanced solutions among technical, economic, and environmental criteria.

Within this context, the multi-objective design approach illustrated in Figure 1(b) is regarded as a highly promising direction. The main steps of the proposed design framework are explained in detail in Sections 2.2–2.4.

2.2. Construction and validation of predictive models for each objective

The first step of the procedure is to collect data for developing predictive models for each performance indicator. Data sources may originate from multiple channels, including laboratory or field experiments, numerical simulations, or existing databases from previous studies, which can be accessed from reliable open repositories such as Mendeley, NIST, and RILEM, or compiled directly from the authors' own research.

Based on the prepared dataset, predictive models are then established to represent the relationships between input variables and each output indicator. Let the set of input variables be denoted as $X = (x_1, x_2, \ldots, x_n)$.

The predictive models provide corresponding outputs $f_i(X)$ for each indicator i. Various approaches can be adopted for model development, including traditional analytical relationships derived from mechanical models, numerical simulations, linear or nonlinear regression methods, and, in particular, modern machine learning techniques such as Random Forest, Support Vector Regression, and Gene Expression Programming [11]. The choice of method depends on the characteristics of the data and the prediction objectives.

After development, the predictive models must be validated to ensure their reliability before being applied in the optimization process. Validation is typically performed by comparing model predictions with experimental results or independent datasets not used during training. Common statistical indicators include correlation coefficients and mean error measures. However, in many cases, reliance on statistical metrics alone is insufficient. Therefore, additional steps such as sensitivity analysis or parametric analysis may be required to assess whether the influence of input variables on each indicator is consistent with the underlying physical mechanisms, thereby enabling more appropriate model calibration. A predictive model is truly useful only when it achieves both high accuracy and compliance with fundamental mechanical principles.

2.3. Definition of design scenarios and constraints

The objective of this stage is to generate a representative and well-controlled set of design alternatives in preparation for the multi-objective optimization process. First, the feasible design space Ω is defined through the set of decision variables of the input parameters $X = (x_1, x_2, \ldots, x_n)$, together with their allowable ranges. Based on these input parameter settings, each output performance indicator $F(X) = (f_1(X), f_2(X), \ldots, f_m(X))$ is calculated for n design scenarios using the predictive model functions previously integrated. However, to ensure practical relevance, constraint conditions must be incorporated for both the input variables and the resulting output indicators.

Input-parameter constraints are limits directly related to the admissible range of each design variable or to the relationships among them. For example, in the design of a typical reinforced concrete beam, the beam width and depth must fall within allowable ranges dictated by architectural requirements and constructability; the reinforcement ratio must exceed a minimum value to prevent brittle failure but not exceed a maximum value to ensure ductility; the bar diameter and spacing must comply with detailing regulations and concrete compaction requirements; the concrete cover thickness must satisfy durability and corrosion protection standards; or the proportion of supplementary cementitious materials replacing cement must not exceed levels that adversely affect long-term durability. These constraints act as "fixed conditions" of the design space, eliminating unrealistic scenarios at an early stage. Input parameters may be defined as continuous variables with boundary conditions $l \le x \le u$; discrete variables defined over a finite set S_k; or categorical variables representing discrete options, which may be encoded when required for predictive modeling. In addition, coupling constraints among variables can also be specified at this stage.

Output constraints are typically imposed in terms of minimum performance requirements that the structure must satisfy. For instance, in structural member design, the flexural and shear capacities must exceed the design demands; instantaneous and long-term deflections must remain within code-specified limits; crack widths must be smaller than thresholds that compromise serviceability or durability; construction cost must not exceed the project budget; and CO_2 emissions over the life cycle of the structure must remain below limits prescribed by environmental regulations. In concrete mix design, technical constraints may include strength, permeability, workability, and durability, in addition to economic and environmental constraints. In general, these constraints function as a "result filter," used to verify and eliminate design scenarios that may be geometrically or materially feasible but fail to meet technical, economic, or environmental requirements.

2.4. Multi-objective optimization

After obtaining the set of design scenarios and the predicted values for each performance indicator, the next step is to perform multi-objective optimization to identify solutions that balance competing objectives. The general problem can be described as follows: find $X \in \Omega$ that simultaneously optimizes $F(X) = (f_1(X), f_2(X), \ldots, f_m(X))$ subject to the constraints imposed on $f_i(X)$. Here, X represents a design scenario defined by a set of design variable values, $f_i(X)$ denotes the value of the i-th objective, m is the number of objectives, and Ω is the feasible design space. Depending on the problem, some objectives are to be minimized (e.g., cost, emissions), while others are to be maximized (e.g., load-carrying capacity, durability). For consistency, maximization objectives are commonly

converted into minimization form by considering $-f_i(X)$. In this way, the entire objective set F(X) can be handled consistently within a unified optimization framework.

Traditionally, weighted-sum methods have been regarded as the most common approach to solving multi-objective problems. In the weighted-sum approach, the problem is reduced to a single-objective function, expressed as

$$F_w(x) = \sum_{i=1}^{m} w_i f_i(x) \text{ with } w_j \geq 0 \text{ và } \sum_{i=1}^{m} w_i = 1 \quad (1)$$

This approach is convenient when the designer has clearly defined the relative importance of each objective. However, the results are often sensitive to the choice of weights wi, and the method may fail to capture the full set of optimal solutions when the objective surface is highly curved or strongly nonlinear.

To overcome the limitations of classical methods, modern population-based search algorithms have been widely adopted due to their ability to explore large design spaces and effectively handle nonlinear relationships. One representative solution is the Non-dominated Sorting Genetic Algorithm II (NSGA-II) [4]. The algorithm starts with a population of candidate solutions $P = (x_1, x_2, \ldots, x_n)$, which are then ranked according to their degree of non-domination (Pareto optimality). In other words, a design scenario X_a is said to dominate X_b if all objective values satisfy $f_j(X_a) \leq fj(X_b)$ for all j, and there exists at least one objective k such that $f_k(X_a) < f_k(X_b)$.

For example, if the objectives are to reduce cost, reduce CO_2 emissions, reduce deflection, and increase flexural capacity, a solution X_a is considered superior to X_b if it is no more expensive, emits no more CO_2, has no greater deflection, provides no less flexural capacity, and is strictly better in at least one criterion, such as lower emissions. Solutions that are not dominated by any other form the best solution set, known as the Pareto front. When selecting parents to generate new generations, NSGA-II combines Pareto ranking with a diversity measure (crowding distance) to simultaneously drive the population toward better solutions and maintain an even distribution. Through iterative crossover and mutation, the algorithm typically produces a diverse set of solutions, offering multiple trade-off scenarios among cost, emissions, and performance for designers to select according to practical priorities.

In this study, NSGA-II is used to solve the constrained multi-objective optimization problem associated with the design of reinforced concrete beams with precast permanent formwork. The algorithm evaluates candidate designs based on structural performance, material cost, and CO_2 emissions, gradually converging toward a diverse set of optimal design solutions.

Since the Pareto front represents multiple equally rational solutions rather than a single optimum, a post-processing step is applied to identify a representative compromise design. The objective values are first normalized using min-max scaling:

$$N(x) = \frac{(x - \min(x))}{(\max(x) - \min(x))} \quad (2)$$

For maximization objectives, the normalized values are transformed using (1 - norm(x)) so that all objectives follow a consistent "smaller-is-better" interpretation. The compromise solution is then determined as the design with the minimum Euclidean distance to the ideal objective point:

$$D = \sqrt{N_C^2 + N_E^2 + (1 - N_F)^2} \quad (3)$$

where N_C, N_E, and N_F denote the normalized cost, CO_2 emissions, and structural performance (specifically the cracking moment, yielding moment, and ultimate moment), respectively. The solution with the smallest D represents the best balanced trade-off among the considered objectives.

Another variant of genetic algorithms is SPEA2 (Strength Pareto Evolutionary Algorithm 2). Similar to NSGA-II, SPEA2 performs selection based on the principle of non-domination; however, instead of relying solely on rank and diversity distance, it assigns each solution a strength index $S(X_i)$. Solutions with larger $S(X_i)$ values are given higher priority, and SPEA2 also maintains an external archive to preserve the best Pareto-optimal solutions. As a result, SPEA2 often converges rapidly toward the optimal front while still ensuring solution diversity.

In parallel with genetic algorithms, swarm-based algorithms have also been widely applied, among which Particle Swarm Optimization (PSO) is a prominent example [12]. Each design solution is regarded as a "particle" with position $X_i(t)$ and velocity $V_i(t)$ at iteration t. During updates, each particle is influenced by its own inertia, its personal best experience, and the collective experience of the swarm, as described by

$$V_i(t+1) = w \cdot V_i(t) + c_1 \cdot r_1 \cdot (p_i - X_i(t)) + c_2 \cdot r_2 \cdot (g - X_i(t)) \quad (4)$$

$$X_i(t+1) = X_i(t) + V_i(t+1) \quad (5)$$

where p_i is the best position previously achieved by particle i, g is the global best solution of the swarm, w is the inertia weight, and c_1, c_2, together with the random numbers r_1, r_2 in [0, 1], control the learning behavior. Equation (2) shows that the new velocity $V_i(t+1)$ is a linear combination of three components: (i) the inertia term $w \cdot V_i(t)$, which prevents abrupt changes in direction; (ii) the term $c_1 \cdot r_1 \cdot (p_i - X_i(t))$, representing attraction toward the particle's personal best experience; and (iii) the term $c_2 \cdot r_2 \cdot (g - X_i(t))$, representing attraction toward the swarm's collective best experience. From a physical perspective, this reflects a balance between inertial forces and guiding forces, analogous to a particle being pulled simultaneously by its own momentum, a "personal magnet," and a "collective magnet." Equation (3) is a simple kinematic update rule in which the new position $X_i(t+1)$ equals the old position plus the displacement induced by the new velocity, similar to basic motion laws in physics. Through these mechanisms, PSO achieves both exploitation of known good solutions and exploration of the design space, aided by the stochastic terms r_1 and r_2, thereby reducing the risk of premature convergence to local optima. When extended to multi-objective optimization (MOPSO), instead of converging to a single global best g, particles select from a set of elite solutions A on the optimal front, causing the swarm to gradually distribute along the Pareto

front. For example, in reinforced concrete beam design, some particles may be attracted toward minimum-cost solutions, others toward minimum CO_2-emission solutions, while many occupy intermediate positions balancing cost, deflection, and load-carrying capacity. Through this mechanism, PSO generates a diverse map of design scenarios, ranging from extremely low-cost to extremely low-emission options, enabling engineers to select optimal solutions under practical constraints.

In summary, for multi-objective optimization problems, traditional weighted-sum methods remain useful when simplicity is desired, and the relative importance of objectives is clearly defined. However, such methods often fail to fully represent the Pareto front, particularly when objective relationships are nonlinear and complex. When a diverse set of solutions is required, and objectives are of comparable importance, genetic algorithms such as NSGA-II or SPEA2 are generally reliable choices due to their robust selection mechanisms and their ability to balance exploitation and diversity. In contrast, PSO offers greater flexibility, with particles moving freely and efficiently exploring the design space, making it suitable for broad initial searches, although it is more sensitive to parameter settings and may exhibit oscillatory behavior that is harder to control.

3. A case study for the design of a reinforced concrete beam with precast permanent formwork

3.1. Design condition description

To illustrate the application of the multi-objective optimization approach in structural design, this study considers a representative case of a reinforced concrete beam incorporating a precast permanent formwork, as shown in Figure 2 [13-15]. Unlike conventional construction methods employing steel, timber, or plastic formwork, where the formwork serves only a temporary role and is removed once the concrete reaches sufficient strength, this type of formwork is prefabricated from concrete itself, with or without reinforcement using stainless steel bars or FRP bars, and remains in place after installation as an integral part of the structural member. Consequently, it functions both as formwork during construction and as a load-carrying and protective component during service. This integration offers the potential to enhance structural capacity and durability, while simultaneously introducing the challenge of selecting an optimal design configuration that balances economic and environmental performance.

To define appropriate design objectives, a reference beam with the dimensions shown on the right-hand side of Figure 2, constructed using the conventional method, is considered. The technical, economic, and environmental indicators of this reference beam are taken as benchmark values for comparison. In the optimization problem, the imposed constraint is that the beam using precast permanent formwork must achieve equal or superior flexural performance (including cracking moment, yielding moment, and ultimate moment) while maintaining material cost (excluding construction cost) and CO_2 emissions that are no higher than those of the reference beam. This principle ensures that the proposed design not only satisfies technical requirements but also delivers economic and environmental benefits compared with the traditional solution.

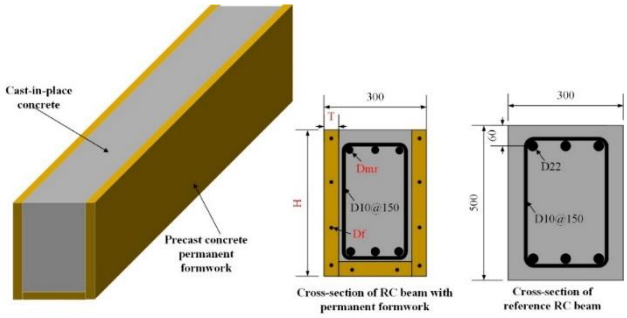

Figure 2. *Reinforced concrete beam using permanent formworks and the reference beam*

The established design parameters are summarized in Table 1 and are divided into three groups: (i) a set of fixed parameters, including the material properties of the cast-in-place concrete, the main reinforcing steel, and basic geometric characteristics, which are kept identical to those of the reference beam; (ii) a set of design variables representing the allowable ranges for adjusting the overall beam dimensions, the precast permanent formwork geometry, and the presence or absence of internal reinforcement within the formwork, with several inter-variable constraints applied to eliminate unrealistic configurations; and (iii) a set of output indicators comprising mechanical quantities, namely the cracking, yielding, and ultimate moments (M_{cr}, M_y, and M_u), as well as total material cost (C_{total}) and total CO_2 emissions (M_{CO2_total}), all of which are required to meet or exceed the benchmark values of the reference beam.

For (ii) a set of design variables, the compressive strength of the formwork concrete is defined in the range of 30–150 MPa with an increment of 10 MPa. Correspondingly, the tensile strength is constrained to be one-tenth of the compressive strength, resulting in a range of 3–15 MPa. The upper bound of the compressive strength of the permanent formwork concrete (150 MPa) is considered because the formwork layer is relatively thin and remains as part of the structural member; therefore, the use of such high-strength precast concrete is technically feasible and has been adopted in several experimental studies on permanent formwork systems. In addition, the reinforcement embedded in the permanent formwork is represented by two material families: steel reinforcement and FRP reinforcement. In the model, coupling constraints are imposed between the elastic modulus and the strength parameters of these materials. Specifically, for steel reinforcement, the elastic modulus, yield strength, and ultimate tensile strength are defined as 210 GPa, 450 MPa, and 694 MPa, respectively. For FRP reinforcement, the elastic modulus is taken as 70 GPa, and both the yield strength and tensile strength are assumed to be 2000 MPa. This assumption reflects the typical brittle behavior of FRP materials, which usually fail directly upon reaching their tensile strength without undergoing a distinct yielding

stage. Regarding the selected range of the formwork thickness, values of 0 (without permanent formwork), 20 mm, and 40 mm were considered in this study, while larger values, such as 60 mm, were intentionally not included. This is because the authors aimed to avoid a formwork thickness exceeding the concrete cover thickness of the main reinforcement in the cast-in-place beam (which is typically about 50–60 mm according to common design codes), as this could affect the placement position of the main reinforcing bars.

Table 1. *Design basic parameters and conditions*

Item	Symbol	Range / Value	Unit	Description
Fixed parameters	f_{cc}	30	MPa	Compressive strength of cast-in-place concrete
	f_{tc}	3	MPa	Tensile strength of cast-in-place concrete
	E_{cc}	30,000	MPa	Elastic modulus of cast-in-place concrete
	E_{cf}	32,000	MPa	Elastic modulus of formwork concrete
	f_{ymr}	420	MPa	Yield strength of the main reinforcement
	f_{tmr}	620	MPa	Ultimate tensile strength of the main reinforcement
	E_{smr}	210,000	MPa	Elastic modulus of the main reinforcement
	k_{2mr}	0.01	–	Strain-hardening parameter of the main reinforcement
	r_{stir}	0.002	–	Volumetric ratio of stirrups (0.2% of concrete volume)
	b	60	mm	Concrete cover thickness
	W	300	mm	Beam width
	n_{mr}	6	–	Number of main reinforcing bars
Design variables	f_{yg}	450; 2000	MPa	Yield strength of formwork reinforcement (steel, FRP)
	f_{tg}	694; 2000	MPa	Ultimate tensile strength of formwork reinforcement
	E_{sg}	210, 70	GPa	Elastic modulus of formwork reinforcement
	f_{cf}	−150 to −30	MPa	Compressive strength of formwork concrete
	f_{tf}	3 to 15	MPa	Tensile strength of formwork concrete
	H	350 to 520	mm	Total beam depth
	D_{mr}	18 to 22	mm	Diameter of main reinforcement
	T	0; 20 to 40	mm	Formwork thickness; constraint T < b
	D_g	0 to 13	mm	Diameter of formwork reinforcement; constraint Dg < T/3
Output objectives	M_{cr}	≥ 44.73	kN·m	Cracking moment ≥ reference beam
	M_y	≥ 191.88	kN·m	Yielding moment ≥ reference beam
	M_u	≥ 218.74	kN·m	Ultimate moment ≥ reference beam
	C_{total}	≤ 26.8	USD/m	Material cost per meter of beam
	$M_{CO_2\text{-total}}$	≤ 132	kg CO_2/m	CO_2 emissions per meter of beam

Regarding the selected range of the formwork thickness, values of 0 (without permanent formwork), 20 mm, and 40 mm were considered in this study, while larger values, such as 60 mm, were intentionally not included. This aimed to avoid a formwork thickness exceeding the concrete cover thickness of the main reinforcement in the cast-in-place beam, as this could affect the placement position of the main reinforcing bars. In addition, steel, stainless steel, and FRP were materials for the reinforcement in formwork. Depending on the specific requirements, for structural members exposed to outdoor environments with more aggressive conditions, stainless steel or FRP reinforcement may be more suitable to ensure the long-term durability of the structure. In contrast, conventional steel reinforcement may remain a feasible option when cost efficiency is prioritized, particularly for structural members located inside buildings and less affected by environmental exposure. Furthermore, the diameter range of the reinforcement embedded in the formwork was defined as 0–13 mm, with the constraint that the diameter must always be smaller than one-third of the formwork thickness to ensure practical constructability. For very small reinforcement diameters, for example, around 2 mm, deformed reinforcing bars are generally not available; therefore, welded steel grids with appropriate grid sizes (e.g., 100x100mm) may also be used to improve the bond with the formwork concrete and facilitate practical construction.

In general, the above assumptions can be adjusted depending on the specific constraints and material properties applicable to real projects, and real-world structural design conditions can be considerably more complex. However, since the primary objective of this study is to clarify the application of the proposed multi-objective optimization framework, the design settings have been intentionally simplified as described above.

3.2. Construction of predictive models for objectives and optimization methods

After defining the input conditions and output performance indicators, the analysis framework operates a set of computational modules (predictive models) before optimization, including: a structural analysis module to predict the cracking, yielding, and ultimate moments of the beam; a material cost module to calculate quantities,

volumes, and total cost; and a carbon emission module to estimate emissions from material production, transportation, and construction based on the life cycle assessment (LCA) approach [16]. Only design scenarios that satisfy the output constraints specified in Table 1 are passed to the final stage for optimization using the NSGA-II algorithm [4].

First, the structural mechanics module assumes full composite action between the precast permanent formwork layer and the cast-in-place concrete, with the force equilibrium scheme illustrated in Figure 3(a), based on the authors' previous study [14, 15]. The strain distribution over the cross-section is assumed to be linear: $\varepsilon(y) = -\varepsilon_0 \, y / h_0$, where ε_0 is the strain at the extreme compression fiber, and h_0 is the distance from the compression edge to the neutral axis. Force equilibrium on the cross-section is established by summing the component forces, including compression and tension forces of the cast-in-place concrete, the formwork concrete, the main reinforcing steel, and the reinforcement embedded within the formwork, evaluated over the geometric regions h_0, h_1, …, h_8 as shown in Figure 3(a). Concrete and steel materials are described using nonlinear constitutive relationships, as illustrated in Figure 3(b). For the three critical states (cracking, longitudinal steel yielding, and compression failure), the parameter set $\varepsilon 0$ and the values h_0–h_8 are obtained numerically by solving a system of 10 coupled equations to satisfy force equilibrium, from which the moments M_{cr}, M_y, and M_u are derived. The results obtained from this module have been validated through comparison with experimental results reported in previous studies [17, 18].

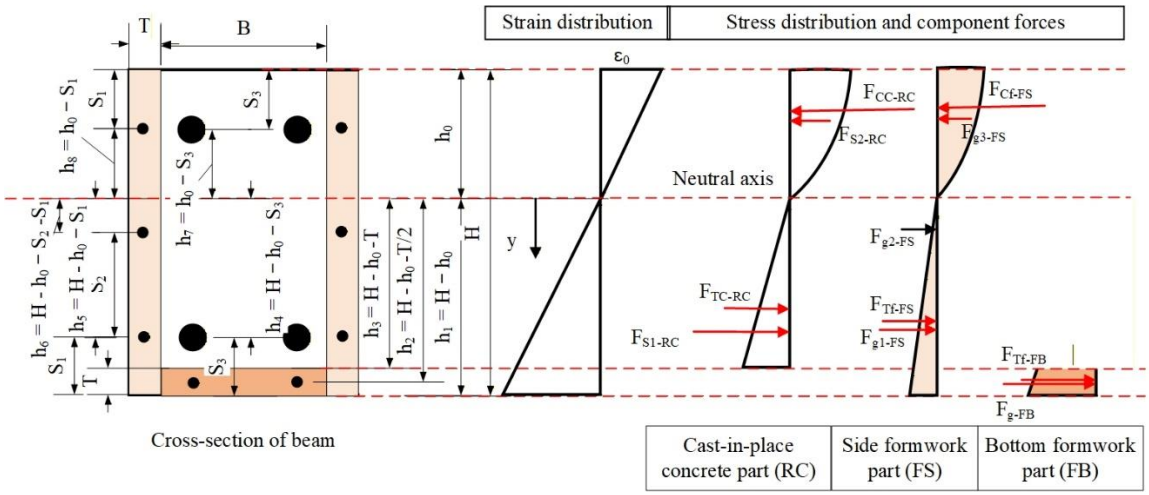

(a) Force equilibrium scheme in the beam cross-section

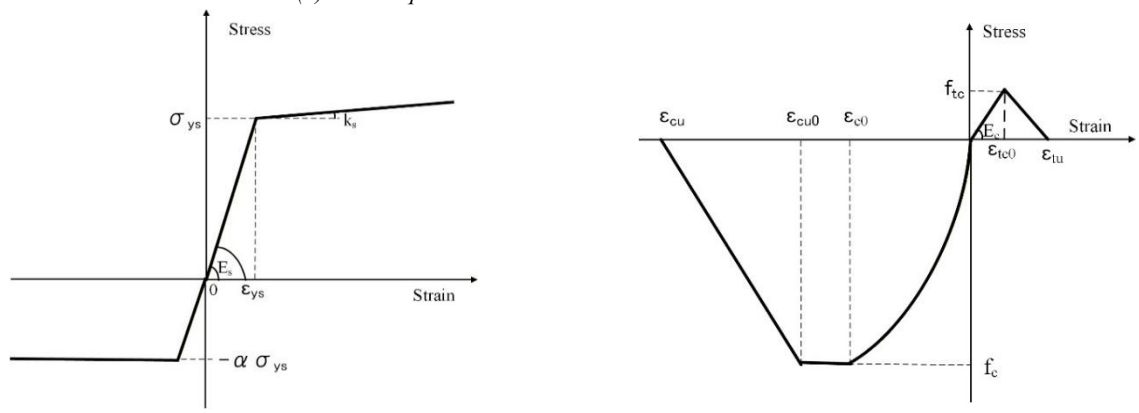

b) Nonlinear material models for concrete, reinforcing steel, and reinforcement

Figure 3. *Theorecal models for evaluating critical moment capacities of the beams*

Next, the material cost module is calculated in a simplified manner based on the volume and mass of each material component corresponding to each design scenario, from which the total cost per meter length of the beam is determined. The general formulation is expressed as:

$$C_{total} = V_{c\text{-}RC} \cdot P_{c\text{-}RC} + V_{c\text{-}F} \cdot P_{c\text{-}F} + m_{s\text{-}RC} \cdot P_{s\text{-}RC} + m_{s\text{-}F} \cdot P_{s\text{-}F} \quad (4)$$

where, $V_{c\text{-}RC}$ and $V_{c\text{-}F}$ are the volumes of concrete in the main beam and the formwork, respectively; $m_{s\text{-}RC}$ is the mass of the main reinforcement and stirrups; $m_{s\text{-}F}$ is the mass of reinforcement within the formwork; and $P_{c\text{-}RC}$, $P_{c\text{-}F}$, $P_{s\text{-}RC}$, and $P_{s\text{-}F}$ are the corresponding unit prices. Although unit prices are fixed in this illustrative study, they can be varied within reasonable ranges in practice to reflect market fluctuations.

Environmental performance is evaluated through CO_2 emission estimation based on LCA. Total CO_2 emissions are determined from two main sources: (i) emissions from material production ($M_{CO2\text{-}prod}$) and (ii) emissions during on-site construction ($M_{CO2\text{-}site}$), as follows:

$$M_{CO2\text{-}total} = M_{CO2\text{-}prod} + M_{CO2\text{-}site} \quad (5)$$

Here, $M_{CO2\text{-}prod}$ is calculated as the product of material quantities and their corresponding emission factors obtained from previous studies. $M_{CO2\text{-}site}$ includes emissions from material transportation, manual labor (reinforcement installation, formwork erection, scaffolding, and concrete casting), and construction equipment (pumps and vibrators). The general formulation is:

$$M_{CO_2\text{-site}} = (m_{cRC}\, D_{cRC}\, EF_{mixer} + m_{sRC} D_{sRC}\, EF_{truck} + m_F D_F\, EF_{truck} + m_{sc} D_{sc} EF_{truck}) + (N_{RC} T_{RC} + N_F T_F + N_{sc}\, T_{sc} + N_{cast}\, T_{cast})\, EF_{lab} + (m_{cRC}\, T_{pump}\, EF_{pump} + m_{cRC}\, T_{vib}\, EF_{vib}) \quad (6)$$

where m_{cRC}, m_{sRC}, m_F, and m_{sc} are the masses of cast-in-place concrete, reinforcing steel, precast formwork, and scaffolding; D_{cRC}, D_{sRC}, D_F, and D_{sc} are the corresponding transportation distances; EF_{mixer} and EF_{truck} are emission factors for mixer trucks and freight trucks; N_{RC}, N_{TF}, N_{sc}, and N_{cast} are the numbers of workers; T_{RC}, T_F, T_{sc}, and T_{cast} are labor durations; EF_{lab} is the emission factor per man-day; T_{pump} and T_{vib} are the durations of pumping and vibration, with EF_{pump} and EF_{vib} being the emission factors of the corresponding equipment. Labor-related parameters and operation times are estimated based on site experience and consultation with construction engineers.

Based on the dataset of design scenarios, including input parameters and the corresponding outputs from the three modules, scenarios are screened using the output constraints specified in Table 1. The remaining dataset is then used for the multi-objective optimization stage. In this illustrative study, NSGA-II is adopted to identify the Pareto-optimal solution set based on the principle of non-domination, rather than aggregating objectives using a weighted-sum approach. All objective functions are formulated in minimization form as follows:

$$f_1(X) = -M_{cr}(X);\ f_2(X) = -M_y(X);\ f_3(X) = -M_u(X);$$
$$f_4(X) = C_{total}(X);\ f_5(X) = M_{CO2\text{-}total}(X) \quad (7)$$

The evolutionary process proceeds over multiple generations through selection, crossover, and mutation until convergence is achieved. The resulting Pareto solution set can be specified in size according to the designer's needs, allowing flexible selection among trade-offs between structural safety, economic efficiency, and environmental sustainability.

3.3. Results and discussions

Before performing the optimization, a sensitivity analysis was conducted to clarify the relative importance of key design variables with respect to each design objective. Five main variables were considered: beam depth, diameter of the main reinforcing bars, thickness of the permanent formwork, diameter of the reinforcement embedded in the formwork, and compressive strength of the formwork concrete. The results are illustrated in Figure 4. The analysis indicates that, among these variables, the diameter of the reinforcement within the formwork exhibits the strongest correlation with structural performance indicators, particularly in the post-cracking stage, including the yielding moment and ultimate moment. This suggests that this parameter plays a decisive role in load redistribution by sharing tensile stresses with the main reinforcement, thereby enhancing flexural resistance at higher load levels. The diameter of the main reinforcement also shows a positive influence, albeit to a lesser extent, due to its relatively narrow variation range constrained by beam geometry. Both types of reinforcement, however, contribute to increases in cost and CO_2 emissions. In contrast, the compressive strength of the formwork concrete shows a significant influence on the cracking moment but a limited effect on other indicators, which is consistent with the primary function of this concrete layer in controlling surface flexural cracking. Meanwhile, the formwork thickness and beam depth exhibit more multidirectional effects. Increasing the formwork thickness enhances stiffness and load-carrying capacity but also increases material quantity, leading to higher cost and emissions. Beam depth directly affects the effective depth and flexural capacity; however, the influence of these variables is generally supportive rather than dominant.

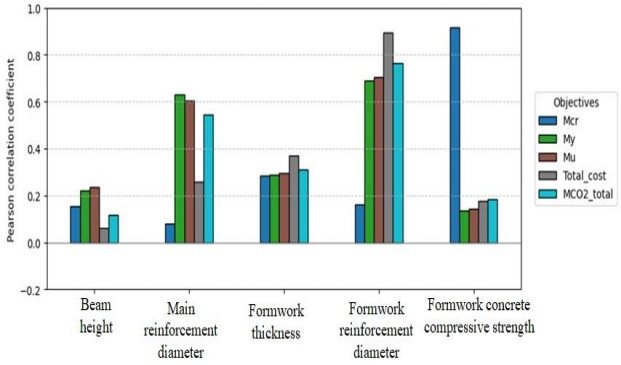

Figure 4. *Results of sensitivity analysis for key design variables*

Figure 5 then presents 20 optimal Pareto solutions selected from 924 design scenarios that satisfy all design constraints, including both input parameters and output performance requirements. Compared with the reference reinforced concrete beam, these solutions exhibit higher moment capacities while simultaneously achieving lower material costs and CO_2 emissions. In addition, the moment values are widely distributed. Some solutions only marginally meet the moment capacity of the reference beam, whereas others demonstrate substantial improvements in structural performance. Many solutions clearly illustrate trade-offs: as moment capacity increases, cost or emissions also tend to increase. Specifically, when structural performance is prioritized, certain designs achieve increases of more than 300% in cracking moment (M_{cr}), along with 20–30% improvements in yielding moment (M_y) and ultimate moment (M_u) relative to the reference beam, although cost and emission indicators are only just within allowable limits. Conversely, when economic and environmental objectives are prioritized, some solutions achieve reductions of 20–30% or more in total material cost (C_{total}) and total CO_2 emissions ($M_{CO2\text{-}total}$) compared with the reference beam, while structural performance remains only comparable to that of the reference beam.

Based on the 20 Pareto-optimal solutions generated using the NSGA-II algorithm, the final design selection can be made according to specific project priorities. In practice,

one objective is often prioritized over others. Accordingly, Table 2 summarizes five representative design solutions optimized with respect to individual priority criteria, including cracking moment, yielding moment, ultimate moment, total material cost, and total CO_2 emissions. It can be observed that, when the cracking moment (Mcr) is prioritized, the selected designs consistently employ permanent formwork concrete with very high compressive strength (approximately 150 MPa) and tensile strength up to 15 MPa. The formwork thickness is typically set at the maximum allowable value of 40 mm. Similarly, when the yielding moment (My) is prioritized, the optimal designs reflect a balanced use of geometry and materials: beam depth and main reinforcement diameter are increased to their maximum values (520 mm and 22 mm, respectively), while the formwork thickness is reduced to 25–35 mm to control total volume and cost. The use of stainless steel reinforcement within the formwork is necessary to enhance yielding resistance. This configuration increases My by approximately 14–27% compared with the reference beam, while material cost increases by only 2–3%, providing a practical balance between performance and efficiency. For ultimate moment (Mu) optimization, the use of FRP reinforcement within the formwork, with an elastic modulus of about 70 GPa (corresponding to GFRP), proves more effective due to its significantly higher tensile strength compared with stainless steel reinforcement. In these cases, the formwork concrete typically exhibits moderate compressive and tensile strengths, ranging from 30–90 MPa and 3–9 MPa, respectively. These solutions reflect a strategy focused on improving post-yield behavior and enhancing structural robustness, allowing Mu to increase by up to 30% while keeping cost and emissions within acceptable limits. In contrast, when material cost or CO_2 emissions are the primary concern, the selected designs tend to shift toward material-efficient configurations. These include moderate beam depth, low-strength formwork concrete (e.g., fc = 30 MPa and ft = 3 MPa), and the absence of reinforcement within the formwork. Although the formwork thickness remains at 40 mm, the elimination of reinforcement and the use of lower-quality concrete significantly reduce cost and emissions. Such solutions can reduce material cost by up to 18% and CO_2 emissions by more than 20%, while still satisfying structural design requirements.

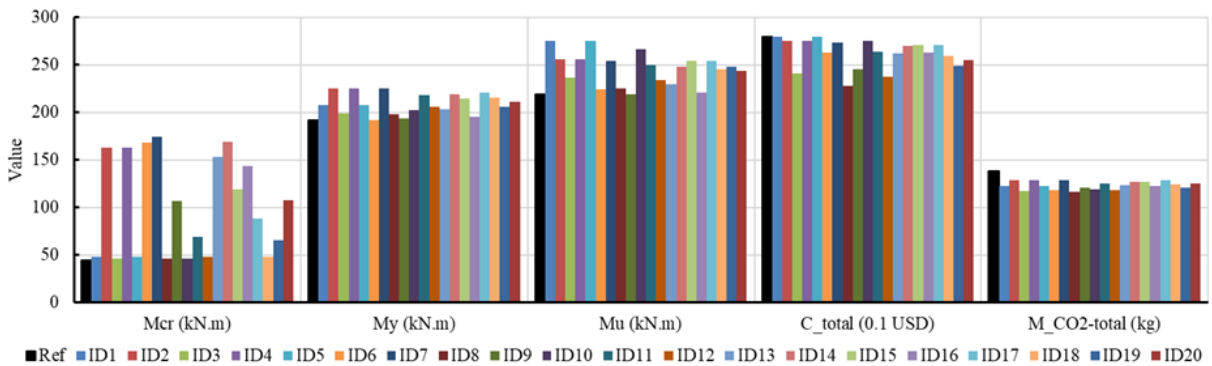

Figure 5. *Results of 20 optimal Pareto solutions*

Table 2. *Optimal design solutions corresponding to individual priority criteria*

Priority criteria	E_{sg} (GPa)	H (mm)	D_{mr} (mm)	T (mm)	D_g (mm)	f_{cf} (MPa)	f_{tf} (MPa)	M_{cr} (kN·m)	M_y (kN·m)	M_u (kN·m)	C_{total} (USD)	$M_{CO_2\text{-total}}$ (kg)
M_{cr}	–	520	22	40	0	150	15	174,4	224,9	254,3	27,3	128,4
M_y	210	520	22	35	2	150	15	162,8	225,5	255,5	27,5	128,9
M_u	70	520	22	20	4	30	3	48,2	207,4	274,9	27,9	122,2
C_{total}	–	510	22	40	0	30	3	46,3	197,7	224,7	22,8	116,2
$M_{CO_2\text{-total}}$	–	510	22	40	0	30	3	46,3	197,7	224,7	22,8	116,1

4. Conclusions

The study has introduced a generalized multi-objective optimization design framework, with a focus on: (i) developing predictive models for each performance indicator based on experimental data, analytical formulations, or machine learning techniques; (ii) defining design scenarios and a system of output constraints; and (iii) applying optimization algorithms to identify the Pareto-optimal solution set, thereby allowing designers to make flexible selections according to priority levels. This framework is becoming increasingly powerful due to the rapid growth of large-scale open-source databases, combined with advances in computational modeling methods, particularly machine learning and numerical simulation. At the same time, progress in modern multi-objective optimization algorithms (such as genetic and swarm-based algorithms) has significantly enhanced the ability to explore complex design spaces and identify balanced solution sets, greatly expanding the potential for application in structural design.

The study also demonstrated the framework through a case application involving the design of an advanced structural system, namely reinforced concrete beams using permanent (non-removable) formwork. The results

indicate that the obtained Pareto front can simultaneously improve structural performance and sustainability compared with the reference beam. When structural performance is prioritized, the cracking moment M_{cr} increases by more than 300%, while the yielding and ultimate moments M_y and M_u increase by 20–30%. Conversely, when economic and environmental objectives are prioritized, the total material cost and total CO_2 emissions are reduced by 20–30%, while the load-carrying capacity remains comparable to that of the reference beam. These findings confirm that the multi-objective optimization approach is not only of academic significance but also highly applicable to practical design problems, providing a spectrum of balanced solutions that flexibly accommodate project-specific priorities and support the pursuit of sustainable construction design.

Acknowledgment: This research is funded by the Vietnam Ministry of Education and Training, Project code B2025-DNA-03.

REFERENCES

[1] L. Deng and X. Zhang, "Low Carbon-Oriented Concrete Mix Optimization Using Ensemble Learning and NSGA-II", *The International Conference on Net-Zero Civil Infrastructures: Innovations in Materials, Structures, and Management Practices (NTZR)*, pp. 575-587, 2024.

[2] Q. Xue, Z. Wang, and Q. Chen, "Multi-objective optimization of building design for life cycle cost and CO2 emissions: A case study of a low-energy residential building in a severe cold climate", *Building Simulation*, Vol. 15, pp. 83-98, 2022.

[3] M. Z. Zakaria, H. Jamaluddin, R. Ahmad, and S. M. Loghmanian, "Comparison between multi-objective and single-objective optimization for the modeling of dynamic systems", *Proceedings of the Institution of Mechanical Engineers, Part I: Journal of Systems and Control Engineering*, vol. 226, no. 7, pp. 994-1005, 2012.

[4] K. Deb, A. Pratap, S. Agarwal, and T. Meyarivan, "A fast and elitist multiobjective genetic algorithm: NSGA-II", *IEEE Transactions on Evolutionary Computation*, vol. 6, no. 2, pp. 182-197, 2002.

[5] C. V. Camp and B. J. Bichon, "Design of space trusses using ant colony optimization", *Journal of Structural Engineering*, vol. 130, no. 5, pp. 741-751, 2004.

[6] X. Zou, C. Chan, G. Li, and Q. Wang, "Multiobjective optimization for performance-based design of reinforced concrete frames", *Journal of Structural Engineering*, vol. 133, no. 10, pp. 1462-1474, 2007.

[7] L. F. Verduzco, "Constructability-based multi-objective optimization with machine learning-enhanced meta-heuristics for reinforcing bar design in rectangular concrete columns", *Structural and Multidisciplinary Optimization*, vol. 68, no. 2, p. 29, 2025.

[8] M. DeRousseau, J. Kasprzyk, and W. Srubar III, "Multi-objective optimization methods for designing low-carbon concrete mixtures", *Frontiers in Materials*, vol. 8, p. 680895, 2021.

[9] M. Wang, M. Du, X. Zhuang, H. Lv, C. Wang, and S. Zhou, "Multi-objective optimization of ultra-high performance concrete based on life-cycle assessment and machine learning methods", *Frontiers of Structural and Civil Engineering*, vol. 19, no. 1, pp. 143-161, 2025.

[10] Q. Qu, Z. Ma, A. Clausen, and B. N. Jørgensen, "A comprehensive review of machine learning in multi-objective optimization", *IEEE 4th International Conference on Big Data and Artificial Intelligence (BDAI)*, pp. 7-14, 2021.

[11] S. R. Vadyala, S. N. Betgeri, J. C. Matthews, and E. Matthews, "A review of physics-based machine learning in civil engineering", *Results in Engineering*, vol. 13, p. 100316, 2022.

[12] H. Borhanazad, S. Mekhilef, V. G. Ganapathy, M. Modiri-Delshad, and A. Mirtaheri, "Optimization of micro-grid system using MOPSO", *Renewable Energy*, vol. 71, pp. 295-306, 2014.

[13] N. M. Hai, S. Fujikura, T. V. Rin, Y. Shinoda, P. H. Nam, N. D. Tuan, M. T. T. Thuy, N. V. Huong, P. N. Phuong, "Experimental and finite element analysis of permanent formwork impacts on flexural failures of reinforced concrete beams", *Engineering Failure Analysis*, vol. 168, p. 109069, 2025.

[14] N. M. Hai, P. H. Nam, S. Fujikura, V. Thay, N. V. Huong, P. N. Phuong, M. T. T. Thuy, "Experimental and theoretical analysis for flexural performance of reinforced concrete beams using UHPC permanent formwork panels embedded with reinforcement grids", *Structural Concrete*, pp. 1-25, 2025.

[15] N. M. Hai, P. H. Nam, D. C. Chanh, S. Fujikura, T. Visal, "A Quantitative Evaluation of Structural Efficiency and CO2 Emission Reduction of Permanent Formwork for Reinforced Concrete Beams", *Construction and Building Materials*, Vol. 499, p. 144066, 2025.

[16] M. Z. Hauschild, "Introduction to LCA methodology", *Life cycle assessment: theory and practice*, pp. 59-66, 2017.

[17] Z. Qiao, Z. Pan, W. Xue, and S. Meng, "Experimental study on flexural behavior of ECC/RC composite beams with U-shaped ECC permanent formwork", *Frontiers of Structural and Civil Engineering*, vol. 13, pp. 1271-1287, 2019.

[18] S. Yin, X. Cong, C. Wang, and C. Wang, "Research on flexural performance of composited RC beams with different forms of TRC permanent formwork", *Structures*, vol. 29, pp. 1424-1434, 2021.